Planetary and Space Science 90 (2014) 90–99

Contents lists available at ScienceDirect

Planetary and Space Science

journal homepage: www.elsevier.com/locate/pss

VUV and mid-UV photoabsorption cross sections of thin films of adenine: Application on its photochemistry in the solar system

Kafila Saïagh *, Mégane Cloix, Nicolas Fray, Hervé Cottin

Laboratoire Interuniversitaire des Systèmes Atmosphériques, LISA, UMR CNRS 7583, Université Paris Est Créteil and Université Paris Diderot, Institut Pierre Simon Laplace, 61 Avenue du Général De Gaulle, 94010 Créteil Cedex, France

ARTICLE INFO

Article history:
Received 5 August 2013
Received in revised form
25 October 2013
Accepted 11 November 2013
Available online 28 November 2013

Keywords:
Adenine
Photochemistry
VUV spectrometry
Absorption cross sections
Astrobiology

ABSTRACT

The photochemistry of an organic compound in extraterrestrial environments is related to its photoabsorption cross sections in the VUV/UV range (<300 nm). Such data, especially in the VUV range (<200 nm) are quite scarce in the literature. This paper presents an experimental setup and associated methodology to measure VUV/UV spectra of thin films of organic molecules. The case of adenine is extensively discussed as an example study. The absorption cross sections spectrum of adenine between 115 and 300 nm is measured from transmission measurements and accurate calculation of the thickness of our samples set thanks to interferometry techniques and infrared spectrometry. From these data, the infrared integrated band strength of solid adenine between 3600 and 1970 cm^{-1} has also been measured and is equal to $7.9\times10^{-16}\pm4\%$ cm molecule^{-1}. The use of the VUV/UV spectrum to estimate the photolysis rate constant is discussed and compared to direct kinetic measurements available in the literature for low Earth orbit experiments. However the lack of measurements of the photodissociation quantum yield as a function of the wavelength prevents a precise calculation. VUV/UV cross section spectrum is yet a necessity to conduct either proper kinetic studies on optically thin samples (less than 2 nm in the VUV for adenine) or an appropriate modeling for optically thick samples.

1. Introduction

The emergence of life is the final stage of complex processes involving liquid water and organic matter. The transition between no-life and life occurred when genetic material began to accumulate and replicate in the Earth's primitive environment. Nitrogen bases, composing RNA and DNA, constitute fundamental building blocks of life and have probably played an essential role in prebiotic chemistry. Thus, many studies concentrate on their origin.

Hydrogen acid (HCN) is a key molecule amongst the different mechanisms proposed that lead to the formation of nulceobases. HCN is a major product of spark discharge (Schlesinger and Miller, 1983), UV radiation (Scattergood et al., 1989) and high-energy laser shocks experiments (McKay and Borucki, 1997) on various gas mixtures. This molecule's key role in prebiotic chemistry has been first identified in Miller experiments (Miller, 1957). During the 1960s, works conducted by Oro and Kimbal showed that polymerization of concentrated HCN solutions heated to 80–90 °C can lead to adenine synthesis in yields up to 0.5% (Oro, 1960; Oro and Kimball, 1961, 1962). Since then, many researches are devoted to the abiotic synthesis of adenine from HCN polymerization in different primitive earth conditions. In 1966, adenine has been produced in 15% yield, so far the highest one, by heating a solution of hydrogen cyanide and liquid ammonia at 120 °C (Wakamatsu et al., 1966). In 1978, Ferris et al. (1978) detected 0.04% adenine from NH_4CN stored in dark at room temperatures for 4–12 months. However, these syntheses require a high ammonia concentration (above 1.0 M), which is not relevant to earth primitive environment (Summers and Chang, 1993). Furthermore, such reactions need high concentration of HCN (above 0.1 M) to compete with hydrolysis to formamide ($HCONH_2$) and formate ion ($HCOO^{2-}$) (Sanchez et al., 1967). It is difficult to reach such concentrations in prebiotic oceans. Stribling and Miller (1987) evaluated HCN concentration in prebiotic oceans as 3.5×10^{-5} M in the most favorable condition of pH and temperature (8 and 0 °C). One way to obtain higher HCN concentration is the eutectic freezing of dilute solutions of HCN (Sanchez et al., 1966). In 1982, adenine has been synthesized by freezing 0.01 M HCN at −2 °C, but at very low yields (0.004%) (Schwartz et al., 1982). Ten times more adenine has been observed from dilute solution of 0.1 M ammoniacal HCN, frozen for 25 years at −20 °C and −70 °C (Levy et al., 2000). Not to mention the limitation of adenine synthesis to restricted locations, it is difficult to believe that such small quantities produced by these methods are significant and sufficient for the formation of the first nucleic acid.

* Corresponding author. Tel.: +33 145176549.
E-mail address: kafila.saiagh@lisa.u-pec.fr (K. Saïagh).

0032-0633/$ - see front matter © 2013 Elsevier Ltd. All rights reserved.
http://dx.doi.org/10.1016/j.pss.2013.11.002

Alternative prebiotic processes not based on HCN chemistry have been proposed for instance, adenine formation may derive from formamide catalyzed by $CaCO_3$ and other inorganic minerals (Saladino et al., 2001). Nevertheless, hydrolysis rates of formamide have been calculated for a wide range of temperatures (30–150 °C) and pH (0–14). Under these conditions steady state concentrations of formamide are very low and do not seem to have a significant role in prebiotic chemistry (Miyakawa et al., 2002).

Thus, the paths toward synthesis of adenine on primitive Earth is still debated and is far from being a consensus in the prebiotic chemistry science community.

An extraterrestrial origin of adenine or at least a contribution is also proposed. Organic material can be delivered to Earth by meteorites, comets and interplanetary dust particles (IDPs) (Chyba and Sagan, 1992).

Carbonaceous chondrites contain up to 3 wt % of organic carbon (for reviews see (Botta and Bada, 2002; Pizzarello and Shock, 2010; Sephton, 2002; Sephton and Botta, 2005). The search of nucleobases content in these meteorites has begun in early 1960s. In 1964, 15 ppm of adenine was detected by Hayatsu et al. in an acetylated HCl-hydrosylate (3 M HCl, 120 °C) of the Orgueil sample using paper chromatography. Since some of the organic compounds could have been altered or destroyed during the acetylation step, the same group analyzed another HCl-hydrolyzed sample of Orgueil in 1968 using the same procedure with no acetylation: 20 ppm of adenine was identified (Hayatsu et al., 1968). Later, the same amount of adenine was found in the Murchison meteorite using mass spectrometry (MS) with more drastic extraction conditions applied (3–6 M HCl or trifluoroacetic acid, $\geq$ 120 °C) (Hayatsu et al., 1975). In 1981, Stoks and Schwartz analyzed water and formic acid extracts of the Murchison, Murray and Orgueil meteorites using gas chromatography, high performance liquid chromatography and mass spectrometry: adenine was respectively identified at concentrations of about 267, 236 and 114 ppb. These concentrations are approximately 100 times greater than the ones reported by Hayatsu (1964) and Hayatsu et al. (1975, 1968). These great discrepancies can be explained in part by the compositional heterogeneity of the meteorite samples: for example, Stoks and Schwartz (1981) have observed large differences between purines concentrations of two samples from the same meteorite. Furthermore, the analytical methods used by Hayatsu (1964) and Hayatsu et al. (1975, 1968), paper chromatography and mass spectrometry are not the most appropriate for a quantitative study in contrast to those used in Stoks and Schwartz (1981) (liquid chromatography). More recently, formic acid extracts of 12 carbonaceous chondrites have been analyzed by liquid chromatography–high resolution mass spectrometry which reflected the wide distribution of adenine in these meteorites: Eleven of them contained this purine in range from 5 to 25 ppb (Callahan et al., 2011).

During the comet Halley flyby missions in 1986, in situ analyses of grains ejected from the nucleus have been done by the VEGA space craft mass spectrometer: PUMA. These measurements might indicate presence of adenine (Kissel and Krueger, 1987) but this detection is highly speculative because of the limited resolution of the spectrometer. Rosetta, a European Space Agency (ESA) mission, will reach and study comet 67P/Churyumov–Gerasimenko in 2014 and will provide more information about the chemical composition of comets and IDPs generated by them.

Micrometeorites (i.e. IDPs fallen on the Earth) are considered as the present day dominant source of extraterrestrial material accreted by the Earth (Love and Brownlee, 1993; Maurette et al., 1995); Bland et al., (1996) estimated the current meteorites flux as $\approx$ 10 t/year whereas dust flux have been estimated as 40,000 $\pm$ 20,000 t/year (Love and Brownlee, 1993). In liquid water, they might have acted as a micro-reactor for prebiotic synthesis (Heidmann et al., 1991). Furthermore, a particular class of them, ultracarbonaceous micrometeorites, contain up to 50% of organic matter (Dobrică et al., 2009).

With respect to meteorites and comets, it is within micrometeorites that organic matter is less protected from solar radiation. The importance of their contribution in organic matter's delivery to Earth is then notably linked to the photochemical stability of organic molecules. In the solar system conditions, the energy essential to chemical evolution is brought by mid-UV and Vacuum UltraViolet (VUV, $\lambda < 200$ nm) radiation. Photochemical studies in the VUV domain and the determination of photolysis constants (J) are then crucial to know the extent of the extraterrestrial contribution of micrometeorites to the origin of life. Nevertheless, some approximations have to be done for the calculation of kinetic data. One of these approximations is the absorption of solid state molecules in the VUV domain. Such absorption spectra are very scarce for organic compounds in the solid state in current literature.

This work presents a methodology to measure VUV cross section absorption spectra of thin organic films. It is developed in the frame of experiments conducted in laboratory and in low earth orbit (LEO) to measure the photostability of organic matter in the VUV (Cottin et al., 2008, 2012; Guan et al., 2010).

How VUV cross section spectrum can be used to derive actual photolysis rate in space is also discussed. Application to adenine is presented in this paper.

2. Material and methods

This section presents the procedure to measure the absorption cross section spectrum of adenine in the VUV domain. Solid organic films are prepared and analyzed using infrared and VUV spectroscopy. From VUV transmission data, the absorption cross section spectra is deduced. Calculation requires an accurate value of the sample's thickness, which has been measured by two independent methods: laser interference technique and interferometric microscopy, both using sample's IR spectra.

2.1. Sample preparation

Samples of adenine are prepared on magnesium fluoride (MgF_2) windows, chosen for their optical transmission properties – they transmit UV down to 115 nm and their cut-off in the infrared domain is at 1000 cm^{-1}. They are inserted in an aluminum cell in order to manipulate them without deteriorating the organic film.

Adenine was purchased from Sigma-Aldrich (purity>99%) and MgF_2 windows were provided by Crystran (thickness: 1 mm, diameter: 9 mm).

The method consists of sublimating molecules and recondensing them on MgF_2 windows. For this, a sublimation reactor has been developed (built by Meca 2000 company, France) (Guan et al., 2010), based on the same concept as the one presented in (Ten Kate et al., 2005).

This system (Fig. 1) is composed by the reactor connected to a pumping system (primary and turbo pump) able to create a vacuum as low as 10^{-4} mbar. The reactor, a cylindrical housing ($\sim$0.1 m^3), contains an oven whose temperature can be set up to 800 °C. A ceramic melting pot containing adenine molecules is placed in this oven above which a carrousel accommodating up to nine cells is hung. Only one of the cells is exposed to the molecules that are sublimated while the others are hidden behind a blinder. Once the organic film deposed reaches the thickness desired, the carrousel can be turned thanks to a handlever situated at the bottom of the reactor and the deposit on the next window begins. The thickness

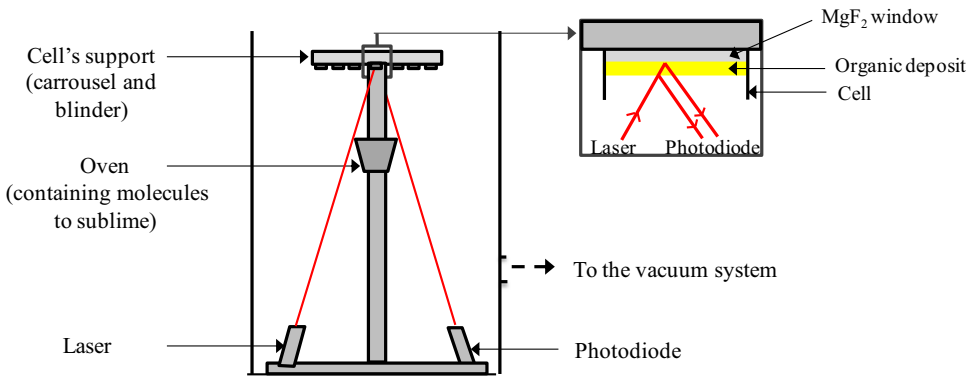

Fig. 1. Schematic view of the reactor, the nine positions sample holder (carrousel) allows a series of eight films (with one blank position), the carrousel is protected by a metal cover (blinder) that has only one opening just in front of the oven.

of the film can be controlled in situ by interferometry thanks to a laser and a photodiode (see Section 2.3.1. for more details).

2.2. Analysis

The transparency of MgF_2 windows to wavelengths in the range of about 115 nm to 10 μm enables transmission measurement in both VUV/ UV and IR domains.

2.2.1. Infrared analysis

The infrared analysis of organic films deposed on MgF_2 windows is measured with an FTIR spectrometer (*Bruker Vertex 70*). The absorption spectra are measured between 4000 cm^{-1} and 1000 cm^{-1} with a resolution of 4 cm^{-1}. Each spectrum is averaged on 32 scans. This analysis allows among others to ascertain that there are no impurities on either the window or the adenine deposit, and that the adenine has not been altered by the sublimation process.

2.2.2. VUV analysis

The VUV spectrometer (*Horiba Jobin Yvon*) (Fig. 2) used to analyze samples has a deuterium lamp as the source of light. This lamp is fitted with a continuous flow of cold water to prevent overheating.

The optical path between this source and the detector comprises

(i) a first optical chamber that focuses the light coming from the lamp on the entrance slit of the monochromator;
(ii) a monochromator H20-UVL (grating: 1200 grooves/mm, dimensions $40 \times 45 \times 7$ mm^3, opening of slits 130–160 μm) covering 100–300 nm range;
(iii) a second chamber which allows focalization of the beam from the exit slit of the monochromator to detector;
(iv) a sample room fitted with a sample holder and a photomultiplier Hamatsu R8486.

The whole system is connected to a pump that provides vacuum conditions to get rid of absorption due to atmospheric O_2. All analyses were concluded at $\approx 7.10^{-5}$ mbar.

The samples holder is a carrousel with eight positions for the samples controlled by an external lever. Then, up to eight cells can be an analyzed in a row, without breaking vacuum.

UV absorption spectra were measured between 115 and 300 nm (lower limit is set by MgF_2 windows on the lamp, the sample and the detector). They were recorded in transmission mode. This measurement is done in two steps: an acquisition between 115 and 230 nm and another in the range of 200–300 nm,

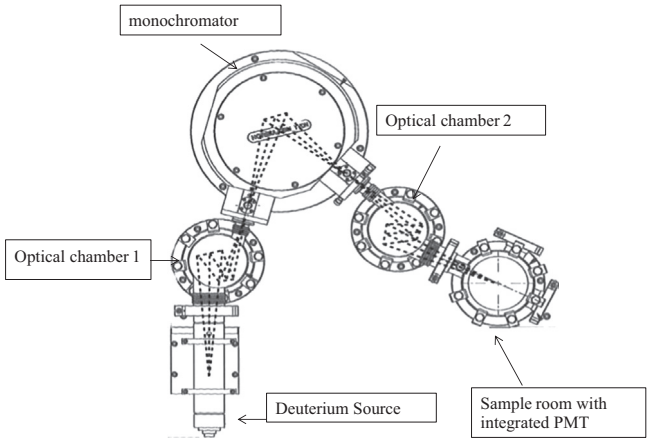

Fig. 2. The beam optical path (in dotted line) of the VUV spectrometer. (Scheme courtesy of Horiba Jobin Yvon.)

for which we used a filter absorbing all the wavelengths lower than 230 nm to avoid 2nd order superposition.

A spectrum of an MgF_2 window without deposit is recorded before each sample and is used as a reference. Thus we obtain the incident (I_0) and transmitted (I_t) intensities from which transmission spectra are calculated.

Photoabsorption cross sections σ (cm^2) of each sample were calculated using the following relation derived from the Beer–Lambert law:

$$\sigma = \frac{1}{N} \times \ln\left(\frac{I_0}{I}\right) \quad (1)$$

With N, column density (molecule/cm^2)

$$N = \frac{z\rho N_a}{M} \quad (2)$$

With z the thickness of the film (cm), ρ is its density, 1.49 g cm^{-3} and (Kilday, 1978), M is the adenine molar mass, 135.13 g mol^{-1}.

2.3. Thickness measurement

2.3.1. Laser interference technique

In this method, measurement occurs during the deposit, in the sublimation chamber, allowing in situ control of the thickness of each sample. The reflected signal from a diode laser (650 nm) directed onto the adenine film was measured using a photodiode as sample is deposited onto the window (Fig. 3). An interference pattern is created from the interference between the light reflected from the window surface and the organic film. The

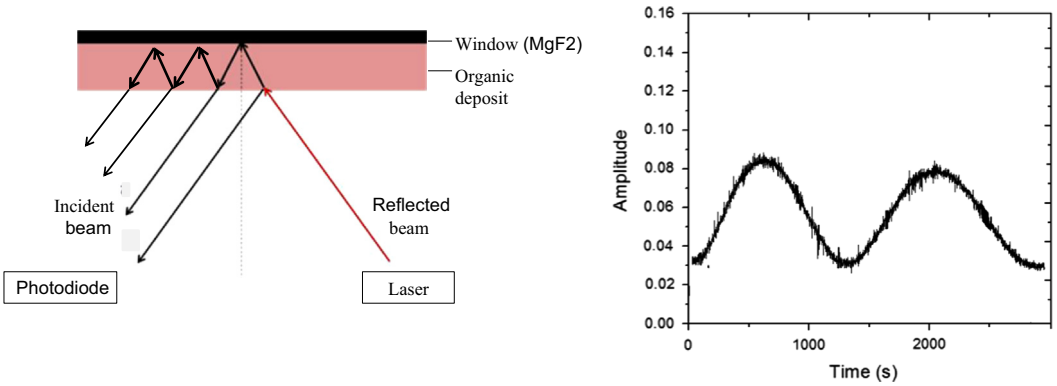

Fig. 3. On the left, schematic explanation of the principle of optical interference observed during the deposit. At one side of the bottom of the reactor, a diode laser emits a light beam (650 nm) which is reflected both by the deposit and the cell's window. A photodiode receives the reflected light and measures variations in intensity related to the thickness of the growing deposits. At the right, typical measurement recorded by the photodiode: a film of two times equal thickness (2 fringes).

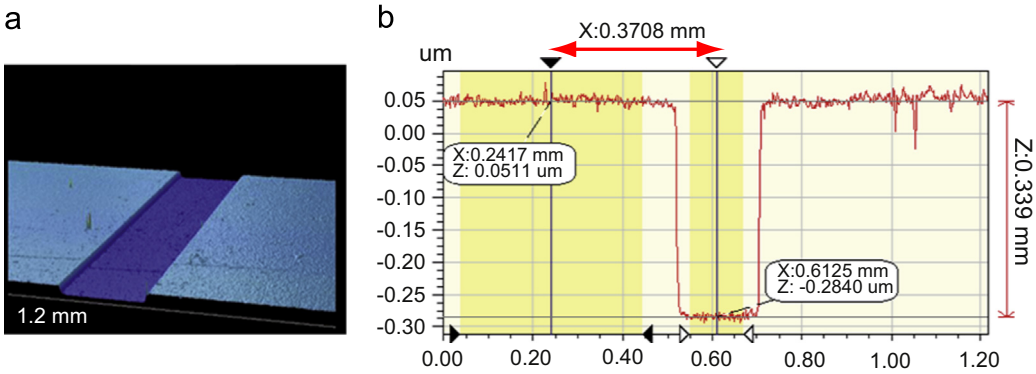

Fig. 4. Example of a thickness measurement with interference microscopy. (a) 3-Dimensionnal image; the color code is linked to the depth. The clear part is the top of the film; the dark part is the trench performed using a hard tip. (b) X profile gives access to the step height and then the sample thickness, here equal to 339 nm. (For interpretation of the references to color in this figure legend, the reader is referred to the web version of this article.)

thickness increasing, the intensity measured by photodiode leads to a profile of interference fringes (Fig. 3).

The thickness of the film is proportional to the number of fringes. Each fringe equals a same thickness value given by Eq. (3), where d is the adenine film thickness for one fringe, λ is the laser wavelength, 650 nm, n is the refractive index of solid adenine at 650 nm, $1.65 \pm 0.6\%$ (Arakawa et al., 1986), and i is the angle of the laser reaching the sample in the experimental setup, $15^{\circ} \pm 1\%$.

$$d = \frac{\lambda}{2n \cos r} \Rightarrow d = 200 \text{ nm} \quad (3)$$

For example, if two fringes are recorded during the deposit, the corresponding sample has a thickness of $2d = 400$ nm.

This method is considered to be a relative measurement linked to n for which we rely on literature (Arakawa et al., 1986). Furthermore, the estimation of the beginning and the end of a fringe is subjective and leads then to imprecision on the thickness value of about 10–20%. In order to get over those limitations, we have combined this method to an absolute one.

2.3.2. Interferometric microscopy

An interferometric microscope (*Wiko NT 1100*) has been used to measure 3D topography of samples with a precision of some nanometers. It is a microscope associated to a Mirau interferometer. A beam emitted by the light source is split into two beams of nearly equal intensity, one of these beams being directed onto a flat reference mirror and the other onto the sample surface. The light produced by reflection of these two beams is then combined to interfere. Then, a two-beam interference pattern is recorded by a camera. From this, 2D and 3D images of the sample are built (Fig. 4).

The measurement of the deposit thickness requires having a step height: to do that, a furrow is traced into the deposit using a fine tip once all the spectra have been measured.

2.3.3. IR spectra

In addition to purity controls, IR spectra are also used to calculate the thickness of samples and more specifically the thinner ones.

Indeed, below a certain thickness of organic deposit, approximately 20 nm, interferometric microscopy is not adapted. Moreover, below a quarter of fringe (50 nm), it is difficult to assess the number of fringe.

However, even the thinner samples used in this study displayed significant infrared features that could be used for thickness estimation. With a good correlation between IR area of a bands pattern, between 3600 and 1970 cm^{-1} (called α-band further in this paper), and thicknesses measured by one method, it is possible to deduce all samples' thicknesses from the IR spectrum, even the thinner ones, for which the laser interference technique and interferometric microscopy methods cannot be used.

3. Results and discussion

3.1. Infrared analysis

The IR spectrum of a film of adenine is shown in Fig. 5. The assignments of the infrared peaks have been performed thanks to (Hirakawa et al., 1985) and (Mathlouthi et al., 1984) and are shown in Table 1.

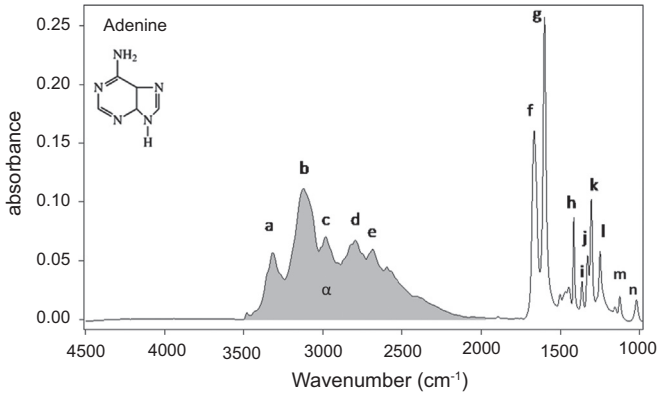

Fig. 5. IR spectrum of solid adenine in the range 4000–1000 cm^{-1}. Gray area is the band pattern called "α band" in this paper.

Table 1
Spectral assignments for the adenine films on a MgF_2 window.

Label	Wavenumber (cm^{-1})	Band assignment
a	3314	$\nu_S NH_2$
b	3122	$\nu_{AS} NH_2$
c	2984	νNH
d	2798	νCH
e	2689	νCH
f	1665	δNH_2
g	1600	νCN
h	1417	δN═C–H
i	1366	δCH
j	1330	νCN
k	1307	νCN
l	1251	δNH
m	1120	νCN
n	1023	δNH2

ν: Stretching and δ: bending (Hirakawa et al., 1985; Mathlouthi et al., 1984).

The assignments of IR bands characteristics of adenine confirm that the heating during the process sublimation does not alter the nature of this compound.

Seventeen adenine samples of various thicknesses have been prepared. The integrity of all of them was checked by infrared spectroscopy and displayed the same spectrum as the one shown in Fig. 6. For each sample, it is thus verified that there was no contamination and that the compound was not degraded during the heating in the sublimation reactor.

3.2. Thickness measurement

For greater clarity, values obtained from the laser interference technique will be called LI thickness and these from the interferometric microscopy IM thickness.

3.2.1. Laser interference technique

LI thickness calculation is based on fringes number measured by photodiode during the deposit in the sublimation reactor, using Eq. (3).

For six samples (0.25–2 fringes), thicknesses have been calculated this way and plotted as a function of the IR α-band area (Fig. 6). A linear regression based on these measurements ($y=2.03$ (± 0.02)) can then be used to calculate the thickness of the thinner samples for which the number of fringes is not defined.

3.2.2. Interferometric microscopy

On samples that are thick enough to be analyzed by interferometric microscopy, two perpendicular furrows have been dug

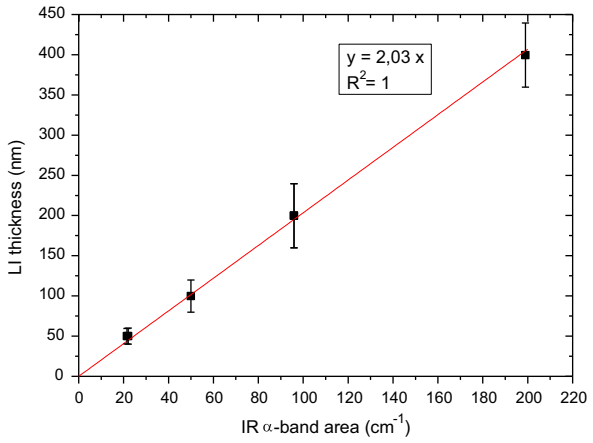

Fig. 6. LI thickness (in nm) (deduced from interference fringes) as a function of IR α-band area (in cm^{-1}).

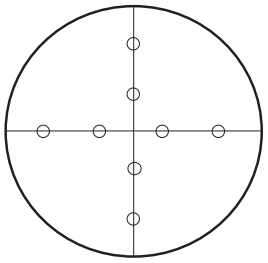

Fig. 7. Thickness measurement by interferometric microscopy on a sample. Each measurement position is indicated by a circle.

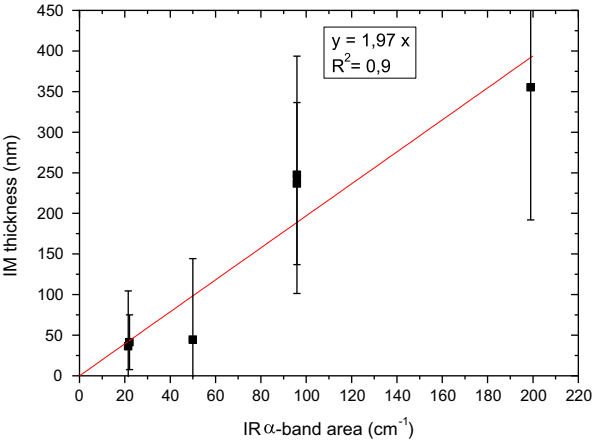

Fig. 8. IM thickness (in nm) measured by interferometric microscopy as a function of IR α-band area (in cm^{-1}).

using a sharp tip. In that case, 80 measurements located at eight different positions (see Fig. 7) are done for each sample.

Thickness is estimated as the average of each measurement on the sample $\pm t_{(n-1)}\sigma$.

With n, the number of measured zones (80), and t, student coefficient at 99% confidence level. This procedure has been implemented on the same six samples measured with the LI method in Section 3.2.1.

Thicknesses of the six samples as a function of IR area band are reported in Fig. 8.

In Fig. 8, IM values are dispersed – it is explained by thickness heterogeneity of adenine deposit along the window. Also, some of them have a bigger dispersion than the others. This is due to their position in the carrousel during the deposit. In fact, MgF_2 windows can be slightly tilted to point the laser beam at the photodiode.

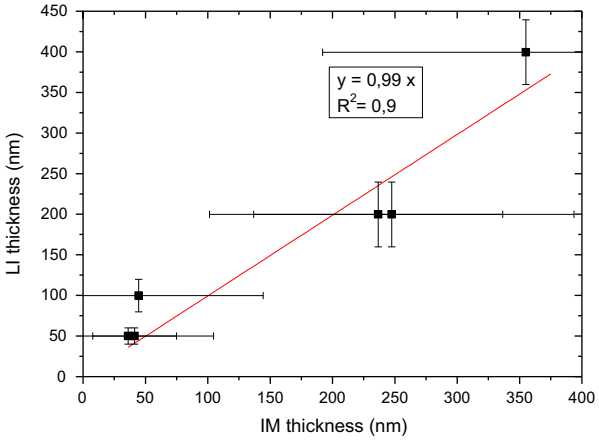

Fig. 9. Comparison of thicknesses of adenine samples measured by LI method and by IM method.

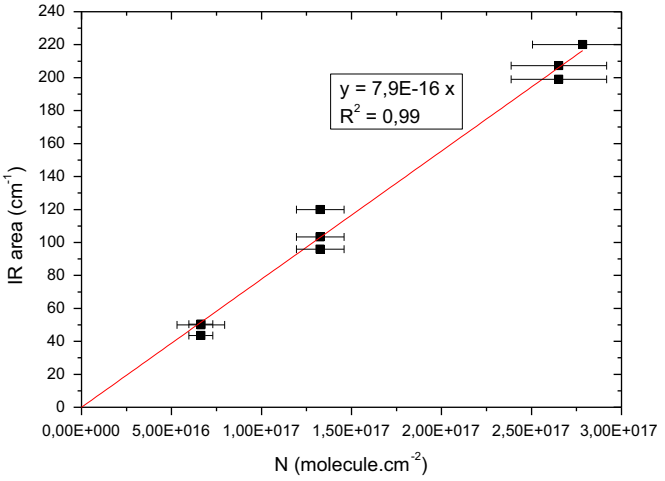

Fig. 10. Calculation of adenine's band strength A (in cm molecules^{-1}) in the band (3600–1970 cm^{-1}).

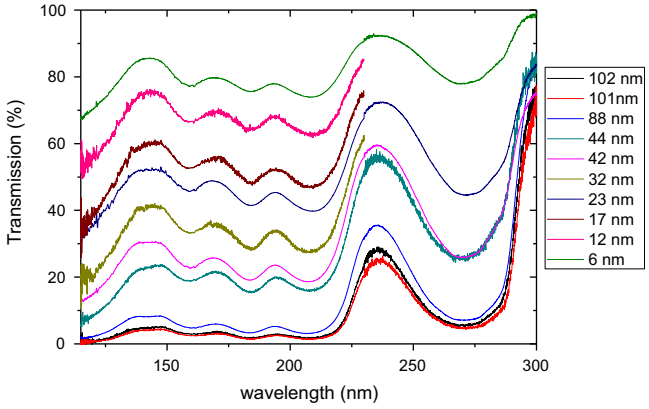

Fig. 11. VUV transmission spectra of adenine films (from 115 to 300 nm) as a function of the wavelengths (nm).

Then the orientation of some windows can be more inclined than the others with respect to the oven containing adenine before the sublimation.

However, many zones of each sample have been measured to ensure the obtaining of a representative average of the film thickness. And, even though a rather large dispersion can be observed, the correlation between IM thicknesses and IR band area is statistically verified with a relative error of 1% (statistic test has been done on the correlation coefficient R). Thus, the equation of linear regression obtained can be also used to extrapolate thickness of thinner samples ($y=1.97(\pm 0.18)$).

3.2.3. Comparison between LT and IM methods

Results of the two thickness measurement methods on the same samples are compared in Fig. 9. Those six samples have both (i) a number of fringe above 0.25 fringes and (ii) a thickness above 20 nm, sufficient to be exploitable by microscopy (see Section 2.3.3).

Fig. 9 shows that IM thicknesses are subject to large uncertainties, due to the relative heterogeneity of the sample (Fig. 8). Measurement by the LI method seems to be more precise but it concerns a restraint zone of the sample, the one reached by the laser during the deposit. This enforces the need for both methods of thickness measurements. Thicknesses measured in this work by the two methods are equivalent (slope$=0.99(\pm 0.08)$). Nevertheless, one of the two methods, the LI one, has a better correlation coefficient ($R^2=1$) than the IM one ($R^2=0.9$). Consequently we chose to use LI thicknesses for the rest of the work.

Moreover, the equivalency of thicknesses values demonstrates the validity of adenine refractive index data found in literature and used for the LI method.

3.3. Infrared band strength

Thanks to thickness measurements, the integrated band strength of solid adenine between 3600 and 1970 cm^{-1} can be calculated from the following equation:

$$A=\frac{\int abs(\sigma)d\sigma}{N} \quad (4)$$

where A is the band strength in cm molecule^{-1}, $\int abs(\sigma)d\sigma$ is the α-band area in cm^{-1} and N is the column density in molecule/cm^2.

Using this equation, the band strength of adenine in the α-band is deduced from Fig. 10. The slope of the linear regression is A equal to 7.9×10^{-16} cm molecule$^{-1}\pm4\%$.

Theoretical IR band strengths of isolated adenine in low temperature Ar matrix have been reported in (Nowak et al., 1996). In the range 3600–1970 cm^{-1}, A is equal to 4.2×10^{-17} cm molecule^{-1}, a value 10 times smaller than the experimental one reported in this work. In the case of adenine, band strength seems to depend strongly on the molecule's physical state and/or temperature.

3.4. VUV analysis

Transmission VUV spectra of adenine film are shown in Fig. 11. Only 10 samples are displayed. Seven samples are too thick and then have negligible transmission. Consequently, these samples are not considered in the rest of the procedure. However, they were essential in the thickness determination step (number of fringe is known and they are measurable by IM).

From each VUV transmission spectrum, the cross section spectra can be deduced. These cross section spectra are calculated using Eq. (1).

The spectra resulting are shown in Fig. 12.

All spectra tend to have the same profile. This highlights the fact that diffusion and reflection are negligible with respect to absorption. A slight dispersion can be observed due to uncertainties during the measurement of thicknesses.

The final spectrum is calculated by averaging of all samples' spectra (Fig. 13).

The absorption peaks at 272, 210 and 185 nm are associated to $\pi\rightarrow\pi^*$ transitions (Polewski et al., 2011; Smith, 1977). The absorption band at 115 nm is a $\sigma\rightarrow\sigma^*$ transition (Arakawa et al., 1986).

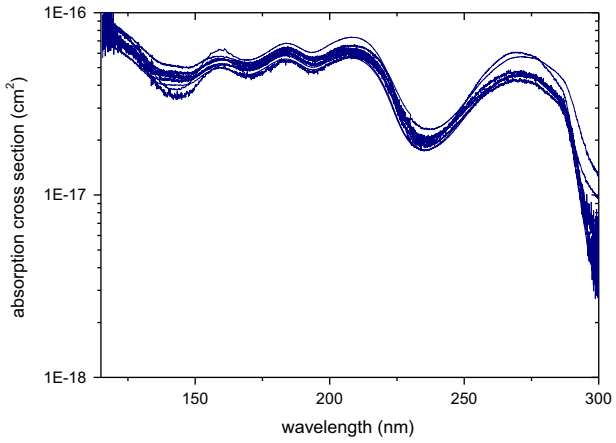

Fig. 12. Absorption cross section (cm^2) of adenine samples (from 115 to 300 nm) as a function of wavelength (nm).

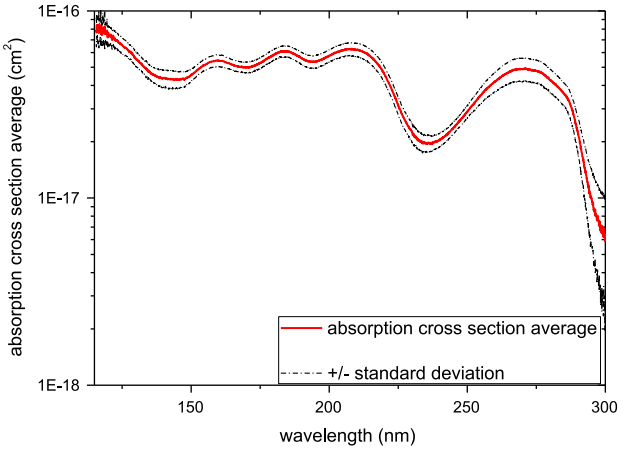

Fig. 13. Absorption cross section (cm^2) of adenine sample (from 115 to 300 nm).

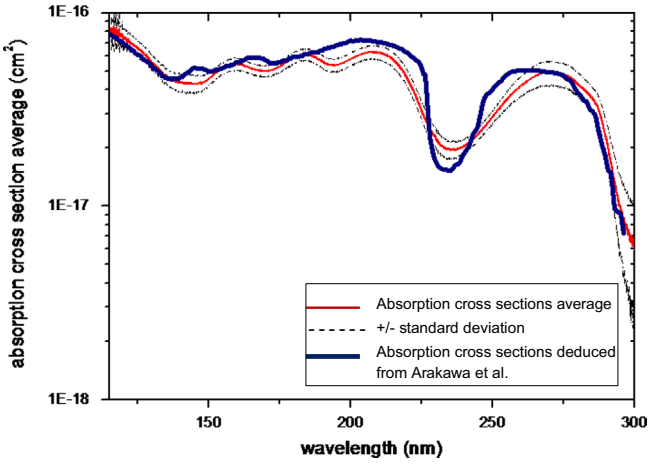

Fig. 14. Absorption cross section of solid adenine calculated from Arakawa et al. (1986) (in blue) superposed to the spectra obtained in this work (in red). (For interpretation of the references to color in this figure legend, the reader is referred to the web version of this article.)

Experimental measurements of the optical reflectance of solid adenine had been obtained for a wide range of wavelengths (Arakawa et al., 1986). The absorption cross section between 115 and 300 nm can be calculated from imaginary part of optical constant provided in these paper using the following equation:

$$\sigma = \frac{4\pi}{\lambda} \times \frac{1}{n} \times k \qquad (5)$$

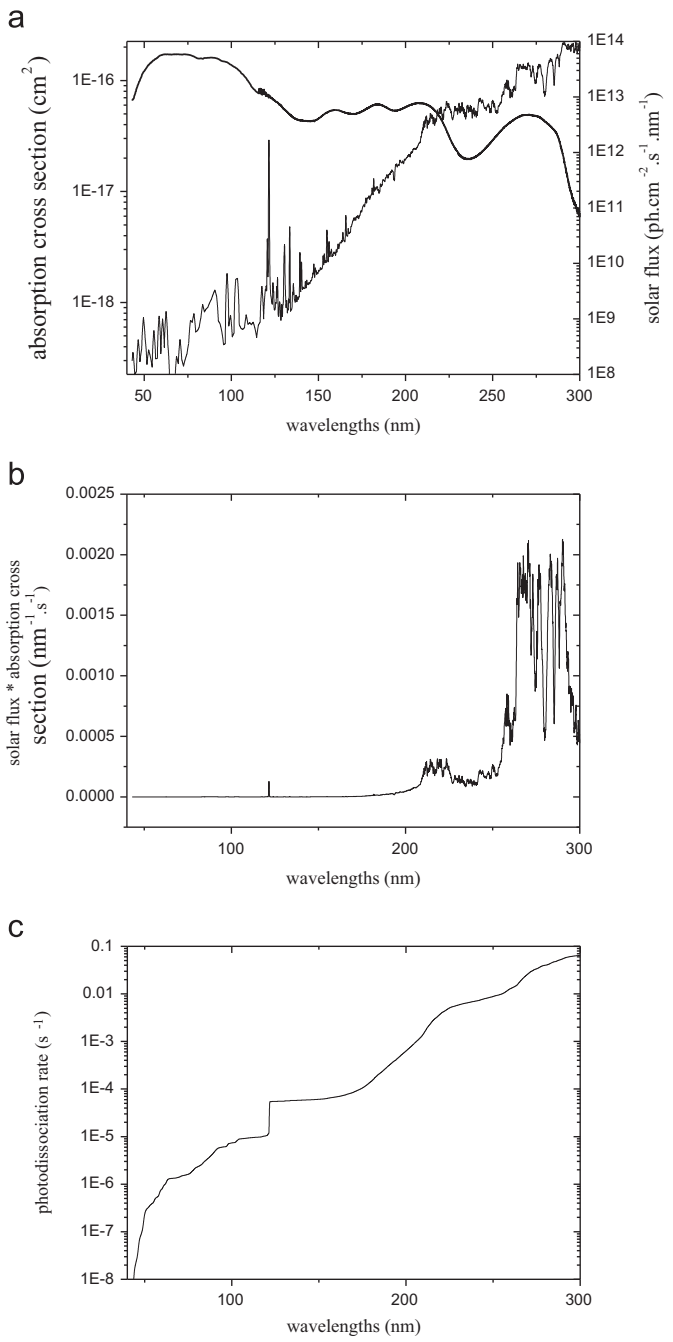

Fig. 15. (a) The solar flux (Thuillier et al., 2004) and the adenine absorption cross section between 40 and 300 nm. (b) Product of solar flux and the cross section from (a). (c) Integrated photodissociation rate J as a function of wavelength (calculation from values presented in (b) with the hypothesis that $\Phi = 1$).

With σ the absorption cross section in cm^2, n in molecule cm^{-3} and k is the imaginary part of the optical constant.

The spectrum calculated is reported in Fig. 14 and compared to our measurements.

Despite a slight deviation (absorption peaks of Arakawa et al. (1986) are roughly 10–15 nm below ours), the good agreement of our experimental values with those obtained from optical data confirms the validity of our procedure. Furthermore, these data can be used to deduce the absorption spectrum of adenine for wavelengths below 115 nm (Fig. 15) which was not considered in our work because of the limitation of MgF_2 transmission.

4. Implications for photochemical models

This section presents an estimation of adenine photolysis constant (J) based on our quantitative measurements of the VUV/UV ($\lambda < 300$ nm) absorption cross section spectra. It is compared to photolysis constant measured from VUV/UV irradiation experiment.

4.1. Photolysis constant calculation from cross section spectrum

The adenine photodissociation rate J can be deduced from the cross section spectrum.

$$J = \int_{\lambda} \sigma_{\lambda} \Phi_{\lambda} I_{\lambda} d_{\lambda} \tag{6}$$

- $I(\lambda)$ is the solar spectral irradiance in photons $cm^{-2}\ s^{-1}\ nm^{-1}$ as a function of the λ. The solar spectra used is ATLAS 1 (solar activity closed to the minimum), given by Thuillier et al. (2004).
- $\sigma(\lambda)$ and $\Phi(\lambda)$ are respectively absorption cross section in cm^2 and the photodissociation quantum yield photodissociaton as a function of wavelength. These two data are intrinsic properties of the molecule and can be measured experimentally in laboratory. However, photodissociation quantum yield is difficult to measure and a very limited amount of data is available in the literature. With no published value for adenine, a rough approximation can be assumed: Φ is equal to 1 in the range where photodissociation can be occuring and 0 above.

Fig. 15 shows how photolysis constant J of solid state adenine can be calculated for a solar UV exposure and how it varies as a function of the assumed wavelength photodissociation limit. Both Arakawa's (for $\lambda < 115$ nm) and this work's data (for $115 < \lambda < 300$ nm) are combined.

A proper assessment of the upper photodissociation limit is critical to calculate. Iizumi et al. (2012) have shown that irradiating adenine in low-temperature argon matrices above 240 nm resulted in that the hydrogen atom of the N–H group was detached from the purine. Otherwise, theoretical studies of adenine molecule concluded that the opening of five-membered ring is double bond of the six-membered ring, which happens above 275 nm, dissipates photons energy and therefore confers purine's intrinsic photostability above this wavelength (Perun et al., 2005). Thus, based on these data, photodissociation threshold is very likely between 240 and 275 nm. Table 2 presents J constant calculated with these two limits.

$J_{(40–240\ nm)}$ is 50% higher than $J_{(40–275\ nm)}$. J thus depends significantly on the photodissociation threshold. To better constrain this data, irradiation experiments should be conducted using cut-off optical filters or a monochromator which would allow choosing radiation wavelength and setting a precise photodissociation limit.

Table 2
Photolysis constants considering two different limits of photodissociation, and with $\Phi = 1$ below this limit.

Limits of photodissocation (nm)	J (s^{-1})
40–240	7.1×10^{-2}
40–275	3.4×10^{-2}

4.2. Photolysis experiments

J can also be measured by photostability studies based on UV irradiation of adenine films and following its UV photodestruction by spectroscopy.

A common approach is to irradiate samples in a vacuum reactor connected to a UV lamp like a microwave-powered H_2 or H_2/He-flow lamp which delivers an emission spectrum dominated in the VUV by the Lyman α band and a wide molecular transition centered at 160 nm (Cottin et al., 2003; Warneck, 1962). But this experimental device does not simulate accurately the actual solar emission.

Another approach is to conduct these experiments in Low Earth Orbit (LEO) where organic molecules are directly exposed to the Sun's emission spectrum (Bertrand et al., 2012; Cottin et al., 2012; Ehrenfreund et al., 2007; Guan et al., 2010).

In both cases, the same method is followed to study the photodestruction of the sample.

4.2.1. Determination of photolysis reaction constant J

The photodestruction reaction of a molecule can be written as

$$A \xrightarrow{h\nu} products \tag{7}$$

With A being a molecule, and products the resulting photoproducts.

If samples are considered as optically thin, the decrease of the molecule's number [A] follows a first order kinetics.

$$\frac{d[A]}{dt} = -J[A] \tag{8}$$

With [A], the number density of A (cm^{-3}) and t the time of irradiation (s).

The integration of Eq. (8) leads to

$$\ln [A]_t = -Jt + \ln [A]_0 \tag{9}$$

The decrease of A can be followed by infrared spectroscopy and J is then experimentally determined thanks to Eq. (9).

Adenine's photolysis constant measured from the LEO experiment is inferior to $1.9 \times 10^{-7}\ s^{-1}$ (Guan et al., 2010).

4.2.2. Limits and discussion

Measuring J experimentally as presented in Section 4.2.1, requires a first order kinetic reaction, which is the case only if the sample is optically thin i.e. if the intensity of the VUV beam transmitted corresponds to 90% of the incident beam.

The thickness of such a sample can be deduced from the absorption cross section of a molecule using the following equation derived from the Beer–Lambert law:

$$z = Ln\left(\frac{I_0}{I}\right) \times \frac{M}{\sigma \rho N_a} \tag{10}$$

With z the thickness of the sample (cm) and σ the absorption cross section of the molecule (cm^2).

Fig. 16 shows the absorption cross section spectra of adenine between 115 and 300 nm and the thickness under which an adenine sample can be considered as optically thin. This thickness is equal to 2–20 nm for the longer wavelengths.

Then, in VUV/UV domain, to allow the measurement of J in a first order kinetics approximation, the adenine sample should not exceed 2 nm.

If the adenine film is not thin enough, the photons flux will depend strongly on the penetration depth. So to deduce J, it is necessary to take into account that the top of the sample will receive a more intense solar flux than the bottom. In this case, it is crucial to calculate J taking into account the radiative transfer

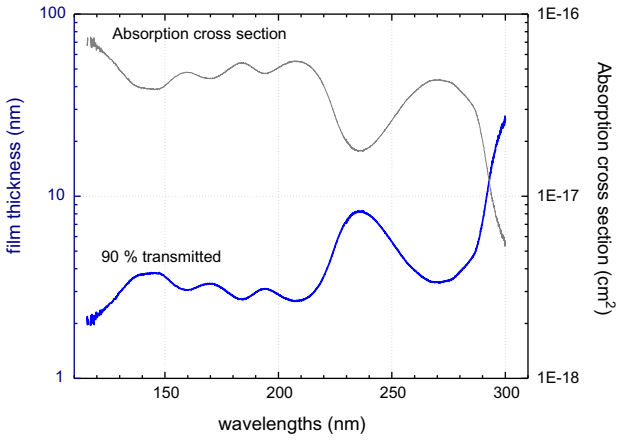

Fig. 16. In blue: dotted line adenine film thickness (cm) under which at least 90% of the incident UV beam is transmitted (115–300 nm). In gray: the absorption cross section (cm^2) between 115 and 300 nm. (For interpretation of the references to color in this figure legend, the reader is referred to the web version of this article.)

Table 3
Summary of the photodestruction rates (s^{-1}) and half-life time at 1 AU from the two methods discussed in text. "LEO" adenine is from samples exposed during UVolution space experiment. "Lab" adenine is adenine samples of the work presented in this article.

	J (s^{-1})	$t_{1/2}$ at 1 AU
Solid "LEO" adenine	$< 1.9 \times 10^{-7}$	>42 days
Solid "Spec" adenine	$3.4 \times 10^{-2} \rightarrow 7.1 \times 10^{-2}$	10 → 20 s

occurring in the sample, knowing the σ that we have measured. Such a modeling is beyond the scope of this paper.

4.3. Results comparison

The two photolysis constants J are presented in Table 3: one calculated using cross section spectra ("Spec" adenine) and one previously obtained from space exposure ("LEO" adenine). An estimation of half-lives resulting from these J at 1 astronomical unit (AU) is also summarized.

Discrepancies between the results reach five orders of magnitude.

A strong limitation of "Spec" adenine J calculation is that the photodissociation quantum yield was fixed to 1 (see Section 4.1). Under this assumption, every photon absorbed by a molecule leads to its photolysis. But other processes, such as (i) fluorescence, (ii) deactivation of the molecule by collision with close molecules (quenching) and (iii) recombination of dissociated adenine, a crucial mechanism in solid state, lead to a significant decrease of the quantum yield. J given in this work thus overestimates the actual photodissociation rate. This is consistent with the smaller "LEO" J resulted from the irradiation of a solid sample, whose photodestruction over time reflects all these intrinsic phenomena. This approach thus avoids the lack of Φ measurements. However, this latter data must also be treated with caution. In fact, "LEO" J has been deduced using first order kinetic from adenine samples which are 200 nm thick (Guan et al., 2010), and thus which are not optically thin. Photon flux reaching molecules located on the upper layers of deposit is greater than the one reaching molecules located in the lower layers. J "LEO" deduced is then probably underestimated. It should then be reconsidered taking into account an appropriate kinetic modeling (see Section 4.2.2). This highlights the importance of modeling the radiative transfer occurring in samples not optically thin. For both methods, a good knowledge of the absorption cross section of the molecule in the VUV/UV range is a prerequisite.

5. Conclusions

VUV and UV radiations are one of the main driving forces for chemical evolution in the solar system. Thus, many photochemical studies are conducted in laboratory to study organic molecules photodestruction rate and hence to determine their life time and their abundance in specific space conditions. Solid compounds studies commonly imply some hypothesis, in particular regarding the absorption cross section spectrum in far UV, data usually unavailable in the literature.

This work aims to enrich these data; this paper focuses on a prebiotic organic compound, adenine, for which VUV and Mid-UV absorption cross section spectrum is measured. This procedure will be used for other organic compounds in the future. Adenine solid films with a known thickness have been analyzed with VUV spectroscopy. Two methods are used to determine samples' thicknesses: (i) a relative method based on the number of interference fringes recorded during the deposit in the sublimation reactor and (ii) an absolute method with interferometric microscopy measurements both correlated with IR spectra. From these data, IR band strength of solid adenine between 3600 and 1970 cm^{-1} has been deduced and is equal to 7.9×10^{-16} cm molecule$^{-1} \pm 4\%$.

The resulting VUV/UV spectrum could be directly used for the calculation of photolysis constant J, knowing integration limits and assuming a quantum yield equal to 1. But such a result has to be considered with caution since it does not take into account all processes involved in the solid film as fluorescence and especially the quenching effect, both leading to less efficient photolysis efficiency. For a better accuracy, J should be experimentally calculated from the monitoring of the photodestruction of a sample as a function of time. Inferring J thanks to this method is quite classical, but it requires the use of a first kinetic order and therefore to study a sample optically thin in VUV and UV domain. The thickness required can be deduced from the absorption cross section spectrum of the molecule which is then a prerequisite for the two methods. This spectrum provides a better knowledge of the sample and notably allows a better preparation of deposits for future Low Earth Orbit experiments.

This work shows that an adenine sample is optically thin in the VUV range under 2 nm. Preparation of such samples is not feasible and not detectable by the analytical techniques we currently use. Then only optically thick adenine samples can be sent in future LEO exposure missions. Kinetic data processing will have to be conducted taking into account the radiative transfer occurring in such samples to deduce an accurate photolysis constant J.

Acknowledgments

This work has been supported by the Centre National des Etudes Spatiales – French Space Agency (CNES) in the frame of the EXPOSE International Space Station Program, IPSL and LISA. K.S. was supported by a grant from the Region Ile de France. Patrick Ausset provided a useful support for interferometric spectrometry. Alain Dutot's advices on statistical treatment of data were appreciated.

Gerard Thuillier is thanked for providing the solar radiation data.

References

Arakawa, E.T., Emerson, L.C., Juan, S.I., Ashley, J.C., Williams, M.W., 1986. The optical properties of adenine from 1.8 to 80 eV. Photochem. Photobiol. 44, 349–353.

Bertrand, M., Chabin, A., Brack, A., Cottin, H., Chaput, D., Westall, F., 2012. The PROCESS experiment: exposure of amino acids in the EXPOSE-E experiment on the International Space Station and in laboratory simulations. Astrobiology 12, 426–435.
Bland, P.A., Smith, T.B., Jull, A.J.T., Berry, F.J., Bevan, A.W.R., Cloudt, S., 1996. The flux of meteorites to the Earth over the last 50,000 years. Mon. Not. R. Astron. Soc. 283, 551–565.
Botta, O., Bada, J., 2002. Extraterrestrial organic compounds in meteorites. Surv. Geophys. 23, 411–467.
Callahan, M.P., Smith, K.E., Cleaves, H.J., Ruzicka, J., Stern, J.C., Glavin, D.P., House, C.H., Dworkin, J.P., 2011. Carbonaceous meteorites contain a wide range of extra-terrestrial nucleobases. Proc. Natl. Acad. Sci. U.S.A. 108, 13995–13998.
Chyba, C., Sagan, C., 1992. Endogeneous production, exogenous delivery and impact-shock synthesis of organic-molecules – an inventory for the origins of life. Nature 355, 125–132.
Cottin, H., Coll, P., Coscia, D., Fray, N., Guan, Y.Y., Macari, F., Raulin, F., Rivron, C., Stalport, F., Szopa, C., Chaput, D., Viso, M., Bertrand, M., Chabin, A., Thirkell, L., Westall, F., Brack, A., 2008. Heterogeneous solid/gas chemistry of organic compounds related to comets, meteorites, Titan, and Mars: laboratory and in lower Earth orbit experiments. Adv. Space Res. 42, 2019–2035.
Cottin, H., Guan, Y.Y., Noblet, A., Poch, O., Saiagh, K., Cloix, M., Macari, F., Jerome, M., Coll, P., Raulin, F., Stalport, F., Szopa, C., Bertrand, M., Chabin, A., Westall, F., Chaput, D., Demets, R., Brack, A., 2012. The PROCESS experiment: an Astro-chemistry Laboratory for solid and gaseous organic samples in low-Earth orbit. Astrobiology 12, 412–425.
Cottin, H.M., Marla, H., Bénilan, Yves, 2003. Photodestruction of relevant interstellar molecules in ice mixtures. Astrophys. J. 590, 874–881.
Dobrică, E., Engrand, C., Duprat, J., Gounelle, M., Leroux, H., Quirico, E., Rouzaud, J.N., 2009. Connection between micrometeorites and Wild 2 particles: from Antarctic snow to cometary ices. Meteor. Planet. Sci. 44, 1643–1661.
Ehrenfreund, P., Ruiterkamp, R., Peeters, Z., Foing, B., Salama, F., Martins, Z., 2007. The ORGANICS experiment on BIOPAN V: UV and space exposure of aromatic compounds. Planet. Space Sci. 55, 383–400.
Ferris, J.P., Joshi, P.C., Edelson, E.H., Lawless, J.G., 1978. HCN: a plausible source of purines, pyrimidines and amino acids on the primitive earth. J. Mol. Evol. 11, 293–311.
Guan, Y.Y., Fray, N., Coll, P., Macari, F.d.r., Chaput, D., Raulin, Fo, Cottin, H., 2010. UVolution: compared photochemistry of prebiotic organic compounds in low Earth orbit and in the laboratory. Planet. Space Sci. 58, 1327–1346.
Hayatsu, R., 1964. Orgueil meteorite: organic nitrogen contents. Science 146, 1291–1293.
Hayatsu, R., Studier, M.H., Moore, L.P., Anders, E., 1975. Purines and triazines in the Murchison meteorite. Geochim. Cosmochim. Acta 39, 471–488.
Hayatsu, R., Studier, M.H., Oda, A., Fuse, K., Anders, E., 1968. Origin of organic matter in early solar system II. Nitrogen compounds. Geochim. Cosmochim. Acta 32, 175–190.
Heidmann, J., Klein, M., Maurette, M., Bonny, P., Brack, A., Jouret, C., Pourchet, M., Siry, P., 1991. Carbon-rich micrometeorites and prebiotic synthesis, Bioastron-omy: The Search for Extraterrestial Life – The Exploration Broadens. Springer, Berlin, Heidelberg, pp. 124–132.
Hirakawa, A.Y., Okada, H., Sasagawa, S., Tsuboi, M., 1985. Infrared and Raman spectra of adenine and its ^{15}N and ^{13}C substitution products. Spectrochim. Acta Part A: Mol. Spectrosc. 41, 209–216.
Iizumi, S., Ninomiya, S., Sekine, M., Nakata, M., 2012. First observation of infrared and UV visible absorption spectra of adenine radical in low-temperature argon matrices. J. Mol. Struct. 1025, 43–47.
Kilday, M.V., 1978. Enthalpies of solution of nucleic acid bases. 1. Adenine in water. J. Res. Natl. Bur. Stand. 83, 348–366.
Kissel, J., Krueger, F.R., 1987. The organic component in dust from comet Halley as measured by the PUMA mass spectrometer on board Vega 1. Nature 326, 755–760.
Levy, M., Miller, S.L., Brinton, K., Bada, J.L., 2000. Prebiotic synthesis of adenine and amino acids under Europa-like conditions. Icarus 145, 609–613.
Love, S.G., Brownlee, D.E., 1993. A direct measurement of the terrestrial mass accretion rate of cosmic dust. Science 262, 550–553.
Mathlouthi, M., Seuvre, A.-M., Koenig, J.L., 1984. F.t.-i.r. and laser-Raman spectra of adenine and adenosine. Carbohydr. Res. 131, 1–15.
Maurette, M., Brack, A., Kurat, G., Perreau, M., Engrand, C., 1995. Were micro-meteorites a source of prebiotic molecules on the early Earth? Adv. Space Res. 15, 113–126.
McKay, C.P., Borucki, W.J., 1997. Organic synthesis in experimental impact shocks. Science 276, 390–392.
Miller, S.L., 1957. The mechanism of synthesis of amino acids by electric discharges. Biochim. Biophys. Acta 23, 480–489.
Miyakawa, S., James Cleaves, H., Miller, S., 2002. The cold origin of life: A. Implications based on the hydrolytic stabilities of hydrogen cyanide and formamide. Orig. Life Evol. Biosph. 32, 195–208.
Nowak, M.J., Lapinski, L., Kwiatkowski, J.z.S., Leszczy, Å., ski, J., 1996. Molecular structure and infrared spectra of Adenine. Experimental matrix isolation and density functional theory study of Adenine ^{15}N isotopomers. J. Phys. Chem. 100, 3527–3534.
Oro, J., 1960. Synthesis of adenine from ammonium cyanide. Biochem. Biophys. Res. Commun. 2, 407–412.
Oro, J., Kimball, A.P., 1961. Synthesis of purines under possible primitive earth conditions. I. Adenine from hydrogen cyanide. Arch. Biochem. Biophys. 94, 217–227.
Oro, J., Kimball, A.P., 1962. Synthesis of purines under possible primitive earth conditions: II. Purine intermediates from hydrogen cyanide. Arch. Biochem. Biophys., 96; , pp. 293–313.
Perun, S., Sobolewski, A.L., Domcke, W., 2005. Photostability of 9H-adenine: mechanisms of the radiationless deactivation of the lowest excited singlet states. Chem. Phys. 313, 107–112.
Pizzarello, S., Shock, E., 2010. The organic composition of carbonaceous meteorites: the evolutionary story ahead of biochemistry. Cold Spring Harb. Perspect. Biol. 2, a002105.
Polewski, K., Zinger, D., Trunk, J., Sutherland, J.C., 2011. Ultraviolet absorption and luminescence of matrix-isolated adenine. Radiat. Phys. Chem. 80, 1092–1098.
Saladino, R., Crestini, C., Costanzo, G., Negri, R., Di Mauro, E., 2001. A possible prebiotic synthesis of purine, adenine, cytosine, and 4(3H)-pyrimidinone from formamide: implications for the origin of life. Bioorg. Med. Chem. 9, 1249–1253.
Sanchez, R., Ferris, J., Orgel, L.E., 1966. Conditions for purine synthesis: did prebiotic synthesis occur at low temperatures? Science 153, 72–73.
Sanchez, R.A., Ferbis, J.P., Orgel, L.E., 1967. Studies in prebiodc synthesis: II. Synthesis of purine precursors and amino acids from aqueous hydrogen cyanide. J. Mol. Biol., 30; , pp. 223–253.
Scattergood, T.W., McKay, C.P., Borucki, W.J., Giver, L.P., van Ghyseghem, H., Parris, J.E., Miller, S.L., 1989. Production of organic compounds in plasmas: a comparison among electric sparks, laser-induced plasmas, and UV light. Icarus 81, 413–428.
Schlesinger, G., Miller, L.S., 1983. Prebiotic synthesis in atmospheres containing CH [4], CO, and CO[2]. II: Hydrogen cyanide, formaldehyde and ammonia. Springer, New York, NY, USA.
Schwartz, A.W., Joosten, H., Voet, A.B., 1982. Prebiotic adenine synthesis via HCN oligomerization in ice. Biosystems 15, 191–193.
Sephton, M.A., 2002. Organic compounds in carbonaceous meteorites. Nat. Product Rep. 19, 292–311.
Sephton, M.A., Botta, O., 2005. Recognizing life in the Solar System: guidance from meteoritic organic matter. Int. J. Astrobiol. 4, 269–276.
Smith, J.J., 1977. The electronic spectrum of purine. Spectrochim. Acta Part A: Mol. Spectrosc. 33, 135–141.
Stoks, P.G., Schwartz, A.W., 1981. Nitrogen-heterocyclic compounds in meteorites: significance and mechanisms of formation. Geochim. Cosmochim. Acta 45, 563–569.
Stribling, R., Miller, S.L., 1987. Energy yields for hydrogen-cyanide and formalde-hyde syntheses – the HCN and amino-acid concentrations in the primitive ocean. Orig. Life Evol. Biosph. 17, 261–273.
Summers, D.P., Chang, S., 1993. Prebiotic ammonia from reduction of nitrite by iron (II) on the early Earth. Nature. 365, 630–632.
Ten Kate, I.L., Garry, J.R.C., Peeters, Z., Quinn, R., Foing, B., Ehrenfreund, P., 2005. Amino acid photostability on the Martian surface. Meteorit. Planet. Sci. 40, 1185–1193.
Thuillier, G., Floyd, L., Woods, T.N., Cebula, R., Hilsenrath, E., Hersé, M., Labs, D., 2004. Solar irradiance reference spectra for two solar active levels. Adv. Space Res. 34, 256–261.
Wakamatsu, H., Yamada, Y., Saito, T., Kumashiro, I., Takenishi, T., 1966. Synthesis of adenine by oligomerization of hydrogen cyanide. J. Org. Chem. 31, 2035–2036.
Warneck, P., 1962. A microwave-powered hydrogen lamp for vacuum ultraviolet photochemical research. Appl. Opt 1, 721–726.